International Journal of Scientific & Engineering Research, Volume 5, Issue 1, January-2014
ISSN 2229-5518

Study of Power and Field Distributions in Induction Heating system by Finite element method

Prof.Dr.Ali K.Al – Shaikhli* , J.A Al – Aboudi , Rana Ali*, Abdullah sahib

*University of Technology , Baghdad

*Baghdad college of economic sciences university, Baghdad

ABSTRACT

To solve the electromagnetic problems of induction heating, there are two main types of solutions. Analytical solution which is limited to one dimensional problems of axially symmetric shapes, and numerical methods which are associated with the advent of digital computers and they can be developed in two dimensions. The finite element method FEM is one numerical methods to give an accurate solution to the given problem.

The objective of paper is to present a normalized solution to reduce the complex calculations efforts with acceptable accuracy and present the results in a general form to be a suitable for more than one particular configuration.

Key-Words: Induction Heating, Electric Fields, Power Distribution, Finite Element Method (FEM) .

الخلاصة

لغرض حل المسائل الكهرومغناطيسية لمنظومات التسخين الحثي ، توجد طريقتان رئيسيتان ، الطريقة التحليلة متمثلة بطريقة الدائرة المكافئة وهي تطبق على مسائل ذات البعد الواحد ، الطريقة العددية التي من الممكن تطبيقها على مسائل ذات البعدين ، طريقة العناصر المنتهية واحدة من اهم الطرق العددية التي تعطى حل دقيق ومفصل لحل المشكلة .

الغرض من البحث هو ايجاد طريقة سهلة وسريعة وعامة من اجل حل المسائل الكهرومغناطيسية لمنظومات التسخين الحثي ، هذا الحل تم تقديمه بصيغة منحنيات عامة ، وقد تم اختبار هذا الحل بمقارنته مع نتائج لبحوث اخرى

International Journal of Scientific & Engineering Research, Volume 5, Issue 1, January-2014
ISSN 2229-5518

Introduction

Power distribution in an inductively heated load is very important for the design of induction heating work coil. The analysis of cylindrical workpieces is relatively straight forward, because they are treated as one-dimensional problem [1]. Serious complexity involves only when dealing with rectangular workpieces which must be analyzed as two-dimensional problem. The application of numerical methods is the only way to solve such problem, there were some attempts to generalize solutions obtained by numerical techniques, they adapted a finite difference scheme to construct a loss chart, to calculate the power in a thick steel plates heated from two sides[2] .

The main objective of this paper is to present a general solution for inductively heated rectangular work pieces by used finite element method, such solution has been given in such a form that it can be used to predict the induction heating system behavior.

Finite element method

The finite element method (FEM) is a numerical technique for solving problems which are described by partial differential equations or can be formulated as functional minimization. A domain of interest is represented as an assembly of finite elements. Approximating functions in finite elements are deter- mined in terms of nodal values of a physical field which is sought. A continuous physical problem is transformed into a discretized finite element problem with unknown nodal values. For a linear problem a system of linear algebraic equations should be solved. Values inside finite elements can be recovered using nodal values. Two features of the FEM are worth to be mentioned [3]:

1) Piece-wise approximation of physical fields on finite elements provides good precision even with simple approximating functions (increasing the number of elements we can achieve any precision).

2) Locality of approximation leads to sparse equation systems for a discretized problem.

System Analysis

Variational Finite Element Method (FEM) is used in the analysis of induction heating system with Quasi-static magnetic field for the configuration as shown in fig (1) along rectangular workpiece (W.P) is positioned inside the heating coil, magmatic field (H) arises on the surface of workpiece .

A thermal insulation and an air gap separate the coil from the workpiece, the system is assumed linear, isotropic and homogeneous with sinusoidal driving current.

The governing equation in two dimensional (x,y) plane may be written as [4]

$$\frac{1}{\mu}\left(\frac{\partial^2 A}{\partial x^2}-\frac{\partial^2 A}{\partial y^2}\right)-\mathrm{J}\omega\sigma A=-J_{\circ} \qquad (1)$$

Where

μ W.p material permeability H/m.

σ W.p material conductivity s/m .

$J_{\circ}$ heating coil current density A/m^2.

A is the magnetic vector potential wb/m.

An element function must be defined in terms of A at the vertices of triangular element as shown in fiq.2

From energy balance criterion, it is found the instantaneous energy supplied by the source must be equal to the instantaneous energy stored in the system enclosed by volume(v).

The energy functional of the system which must be minimized is given by [5]

$$\int_v 0.5[\frac{1}{\mu}\nabla A^2 + J\omega\sigma A^2]\, dv - \int_v J_{\circ} A\, dv \qquad (2)$$

An approximate numerical solution to equation (2), the total energy functional of the system is obtained by collecting G_θ over the total number of element such that:

$$G = \sum_{\theta=0}^{n} G_\theta \qquad (3)$$

Where n is the total number of finite elements.

An approximate numerical solution to the system equation (1) is obtained by differentiating equation (3) with respect to A_i^* for all nodes and equating the derivative to zero, for an Individual node 1 we have :-

$$\frac{\partial G_\theta}{\partial A_i^*} = \sum_{J=1}^{3} S_{ij}\ A_j - T_i \qquad (4)$$

But since the node is common to a certain number of elements(say M element) Then

International Journal of Scientific & Engineering Research, Volume 5, Issue 1, January-2014
ISSN 2229-5518

$$\sum_{\theta=1}^{M} \frac{\partial G_\theta}{\partial A_i^*} = 0 \qquad (5)$$

The assembly of overall stiffness matrix is based on the compatibility of element nodes which means that the nodes when elements are connected the value of unknown nodel variable unity is the same for all elements sharing that node, the consequence of the rule is the basis for the assembly process[6]

By collecting all equation from (4) and summing the corresponding equations as in (5) the system matrix equation will be :-

$$[S] \quad [A] = \quad [T] \qquad (6)$$

Where

[S] is the stiffness matrix (nxn).

[A] is the unknown nodal magnatic vector potentials (1xn).

[S] is the force vector and take values for the coil sub-regions only (1xn)

The surface power density (SPD) can be calculated from the magnetic field intensity (H) . The average power (PAV) supplied to the W.P is [7]

$$H_X = \frac{1}{\mu}\frac{\partial A}{\partial y} \qquad (7a)$$

$$H_y = -\frac{1}{\mu}\frac{\partial A}{\partial x} \qquad (7b)$$

$$\text{PAV} = -\text{Re}[\oint 0.5 \ \{E * H^*\} u \, ds \qquad (7c)$$

Where :

u is a unit vector

for sinusoidal operation the electric field E is given by:

$$E = -\frac{dA}{dt} = -jwA \qquad (8)$$

From equation (7) and (8)

$$\text{SPD} = \text{Real}[0.5 \ \text{jwAH}^*] \qquad (9)$$

Normalization Procedure :

The suggested normalization procedures can be summarized as follows[8]:

1. The variables ω and σ in equation (1) can be replaced with one variable ζ , which incorporates the effect of both variables such as:

$$\zeta = \omega * \sigma \qquad (10)$$

ζ can be maintained constant by changing ω *and* σ simultaneously .

1. The peak value of current density J_o in equation (1) may be taken as unity because, generally, the absolute value of current density is not as important as the value relative to that at the surface.

2. Assuming the half width of work piece in the x-axis is X and in the y-axis Y, Taking x as any point along the work

International Journal of Scientific & Engineering Research, Volume 5, Issue 1, January-2014
ISSN 2229-5518

piece x-axis and y as any point along the work piece y-axis, also let:

$$\overline{\boldsymbol{X}} = x/X \quad (11a)$$
$$\overline{\boldsymbol{Y}} = y/Y \quad (11b)$$

$\overline{\boldsymbol{X}}$ and $\overline{\boldsymbol{Y}}$ take values between 0 and 1 .

Let

$$Y=\lambda*X \quad (12)$$

Where

λ : is constant to be called shape factor ($0 < \lambda \leq 1$)

For λ =1 the W.P takes a square shape (X = Y) and for λ <1 the W.P takes a rectangular shape.

By Substituting equations (6),(10),(11a),(11b) and (12) into equation (1) the system governing equation in two dimensional form will be:

$$\frac{1}{\mu}\left(\frac{\partial^2 A}{\partial \overline{\boldsymbol{X}}^2} - \frac{\partial^2 A}{\boldsymbol{\lambda}^2 \partial \overline{\boldsymbol{Y}}^2}\right) - J\boldsymbol{\zeta}\,\boldsymbol{x}^2 A = -\boldsymbol{x}^2 J_\circ \quad (13)$$

The right hand side of equation (13) represent the peak value of heating coil current density, which is taken as unity.

Let :

$$\tau = \zeta * x^2 \quad (14)$$

$$\eta = \tau * 10^{-7} \quad (15)$$

The quantity 10^{-7} in equation (15) is a scaling factor only, Substituting equations (14) and (15) in equation (13) results:

$$\frac{-1}{\mu}\left(\frac{\partial^2 A}{\partial \overline{\boldsymbol{X}}^2} + \frac{\partial^2 A}{\boldsymbol{\lambda}^2 \partial \overline{\boldsymbol{Y}}^2}\right) + j\eta A = 1 \quad (16)$$

The parameters determine the induction heating system(IHS) behavior governed by equation (16) are η **,** λ and $\boldsymbol{\mu}$. The parameter $\boldsymbol{\mu}$ can be replaced with μ_r as $\mu_\circ$ is constant . hence, a family of curves can be plotted for different values of η **,** λ and μ_r . These curves can be used to determine the behavior of (IHS) following all assumptions made previously.

The results

The work was tested by considering the same data used in reference [9] and listed in Table (1). The result show that when plotting the magnetic field strength along W.P mid –plane axis ,for different . μ_r (maintaining other parameters constants) as shown in fig.(3) there is a significant changes in results for . μ_r lies between 1 and 5 . When . μ_r changed beyond 5 . There is no observable effect. Numerical results show that changing μ_r from 1 to 2 , the normalized mid –

plane magnetic field strength reduced by 37% with respect to that at surface while when μ_r changed from 4 to 5 this field changed by 7% only.

When plotting the magnetic field strength for different values of η (maintaining μ_r and λ constant) there is a range for η values at which the field distribution is very sensitive and the programs develop the same results for η less than 0.1 and more than 1000 . The interpretation of this, is that the depth of penetration δ has the same response for changing μ_r, ω and σ .

Curves for different η and μ_r are shown in figs. 4 to 13 when shape factor λ equal to 0.3 . Using the same principles , other curves for different values of λ can be determined.

The Use of Normalized Curves

The use of the normalized curves is very straight forward. To clarify the extraction of the required information from such curves As an example, consider the same data used [10].which listed in the table (2) and making use of equations(7) to (13) the values of λ is 0.309 and η is 70.14 .

The normalized figure corresponding to the values of λ and $\boldsymbol{\mu_r}$ is fig .4. Results obtained are plotted in Fig.14 and compared with those obtained by [10]. The correlation between the two results is very good and the maximum deviation is about **6%**

Conclusion

Designers and users of induction heating devices need a technique which provide a quick study of induction heating system behavior. This technique should be applied to a wide variety of problems .In this paper a family's of curve has been presented to give a quick study of the influence of various parameter on system performance and determining the best combination to be used in practical design problem. results are verified and design example for the use of the curves are presented

REFERENCES

[1]:Davise E. J. and Simapson, P., "Induction heating handbook" Mcqraw» -Hill, 1979.

[2]: Lim, K. K. , and Hammond, M. A. , " Universal loss chart for the calculation

of eddy-current losses in thick steel plates", Proc. IEE , Vol. 117, No. 4, April 1970.

[3] : G. P. Nikishkov, " Introduction to The finite element method", 2004 Lecture Notes. University of Aizu, Aizu-Wakamatsu 965-8580, Japan

[4]: Ammar Tibouche , Jamil Salhi, Antar bourouina ,"Three-dimensional magneto-thermal model of induction heating process of moving bars",Journées International's de Thermique JITH, Marrakech (Marco), du 13 au 15 November, 2013

[5] : Chari,M.V.K., "Finite elements solution of the eddy current problem in magnetic structures", IEEE Trans, on Power Apparatus system. Vol. PAS-93, 1973, PP. 62-72

[6] : Zienkiewicz, O. C. , "The finite element method in engineering science", McGraw-Hill, Second Edition, 1971.

[7]: Fawzi, T.H., et al., " Boundary Integral Equation Analysis of Induction Devices With Rotational Symmetry ", IEEE Trans, on Mag. , Vol. 19, No. 1, Jan 1983, PP. 36-44.

[8]: Jawad A.alaboudi, "A simplified approach of power and field distributions in induction heating system", Msc.thesis , University of technology, Baghdad,1998

[9]: Ramadhan ,M. , "Boundary element application of induction heating devices with rotational symmetry" ,IEEE,Vol.25,No.4

[10]: Al-Shaikhli, A. K. M., "Power distribution in a rectangular workpieces",IEEE Industry Application

W.P relative permeability	1
W.P conductivity	$3.7 * 10^{-7}$ S/m
Frequency	variable
Coil length	0.32 m
W.P length	0.32 m

Table .1 Data used by [**9**]

W.P half width	0.1737 m
W.P half height	0.0538 m
W.P conductivity	$3.7 * 10^{-7}$ S/m
Frequency	400 Hz
W.P relative permeability	1

Table .2 Data used by [**10**]

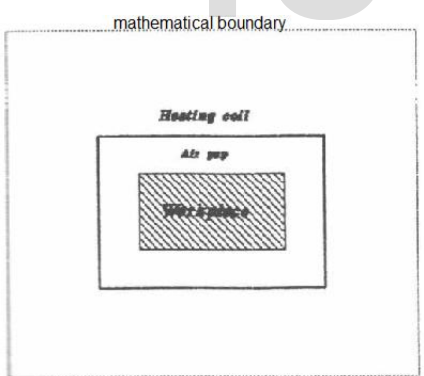

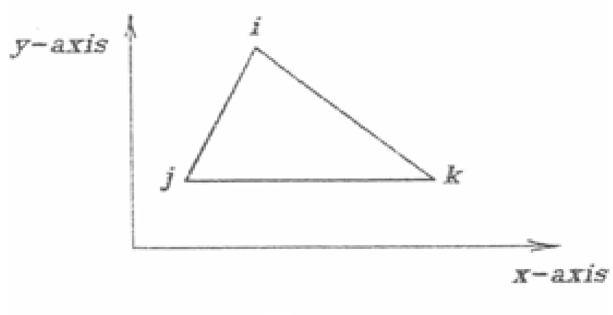

fig .1 Basic induction heating system

fig.2 Typical element

International Journal of Scientific & Engineering Research, Volume 5, Issue 1, January-2014
ISSN 2229-5518

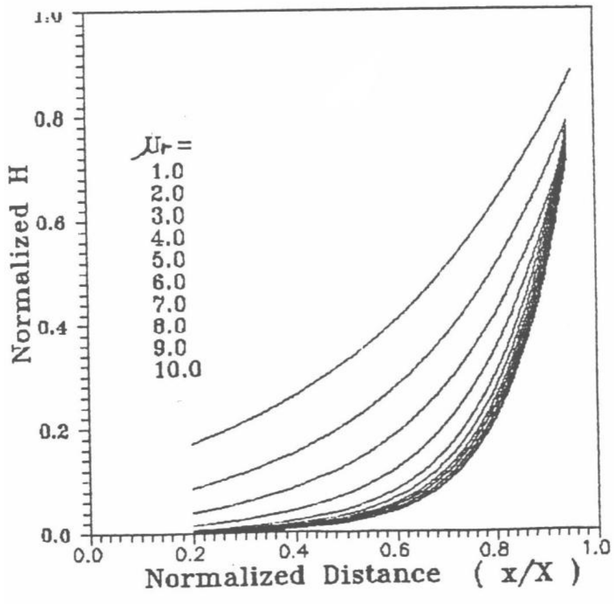

Fig.3 The distribution of normalization H for typical W.P (μ_r varies from 1 to 10)

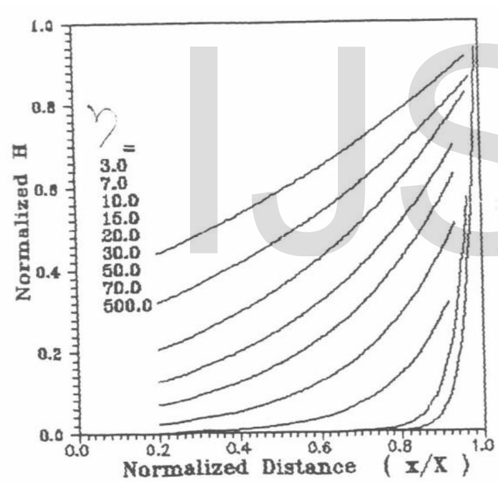

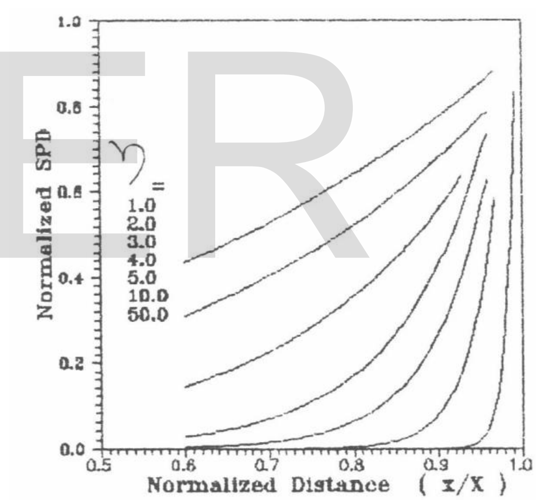

Fig.4 The normalized H distribution for μ_r=1, λ=0.3

Fig.5 The normalized SPD distribution for μ_r=1,λ=0.3

International Journal of Scientific & Engineering Research, Volume 5, Issue 1, January-2014
ISSN 2229-5518

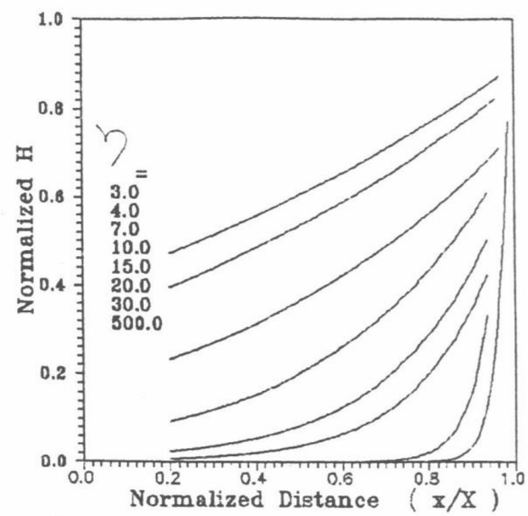

Fig.6 The normalized H distribution for μ_r=2, λ=0.3

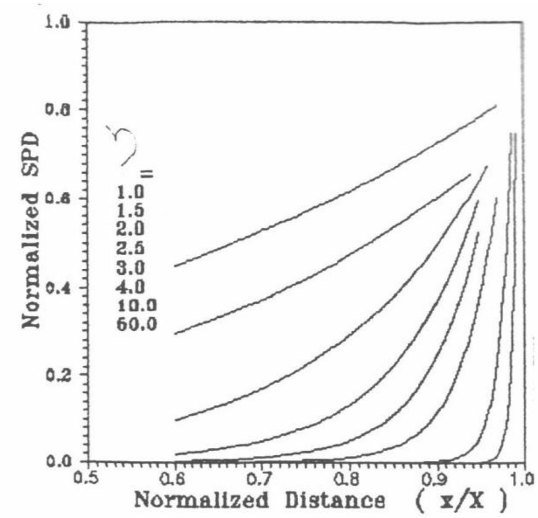

Fig.7 The normalized SPD distribution for μ_r=2,λ=0.3

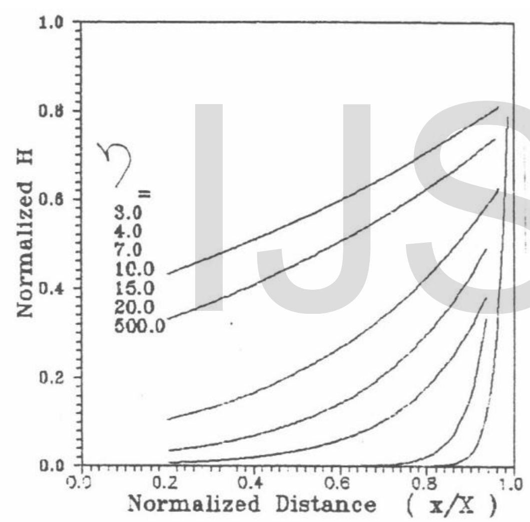

Fig.8 The normalized H distribution for μ_r=3, λ=0.3

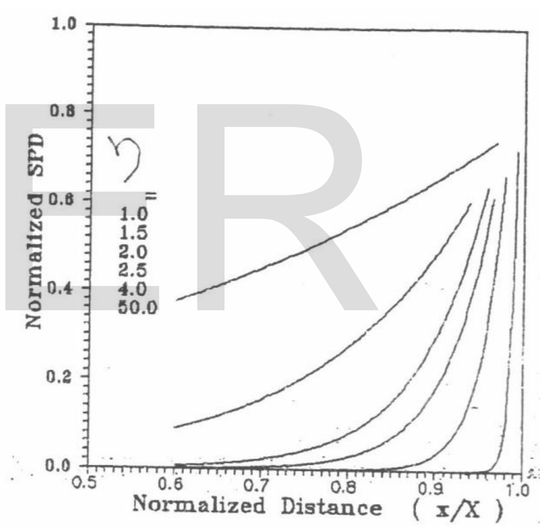

Fig.9 The normalized SPD distribution for μ_r=3,λ=0.3

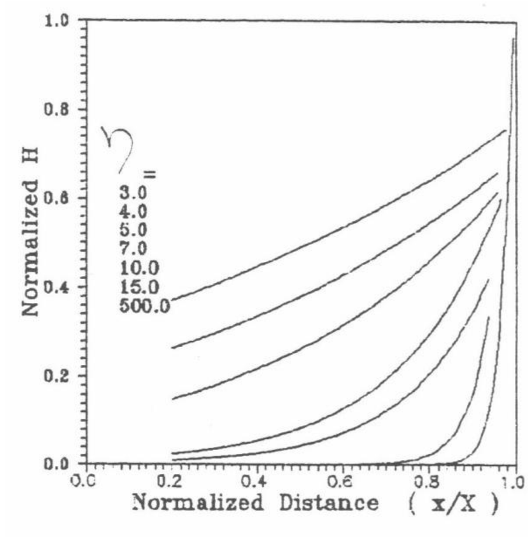

Fig.10 The normalized H distribution for μ_r=4, λ=0.3

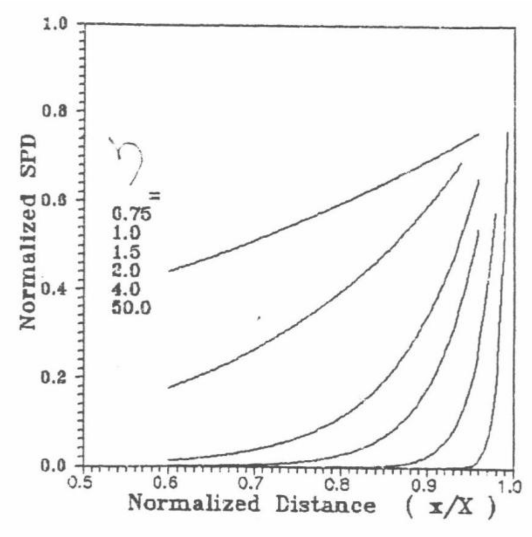

Fig.11 The normalized SPD distribution for μ_r=4,λ=0.3

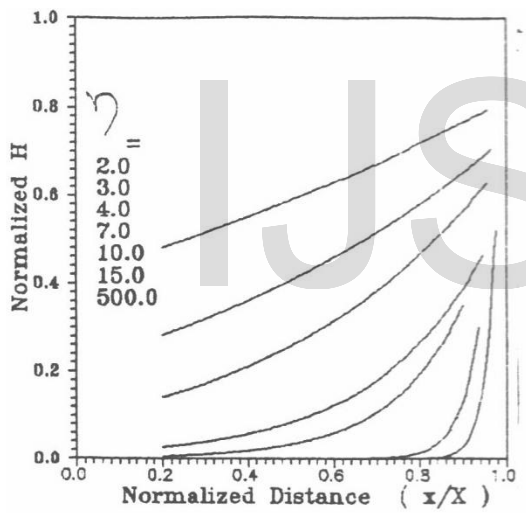

Fig.12 The normalized H distribution for μ_r=5,λ=0.3

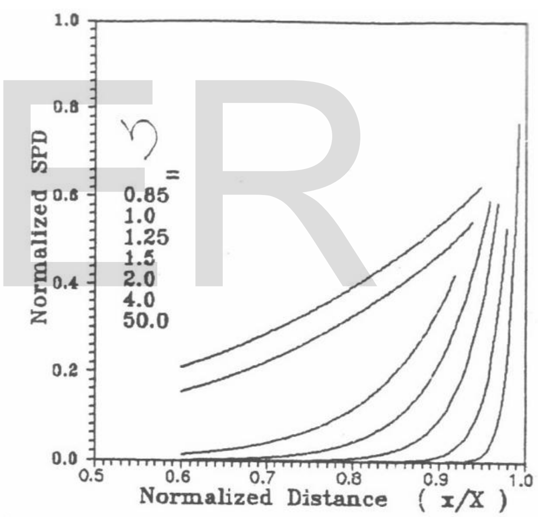

Fig.13 The normalized SPD distribution for μ_r=5,λ=0.3

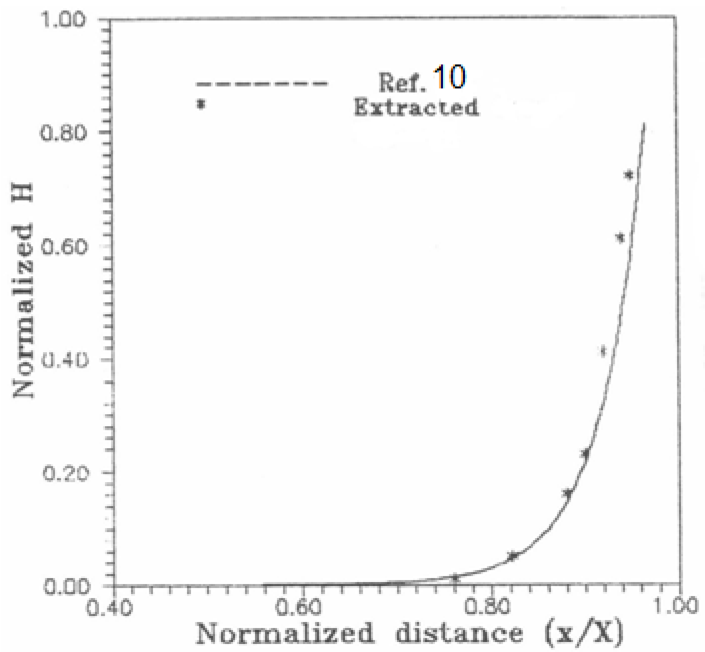

Fig14. The distribution of normalization H compared with that obtained for normalized curves